

Platinum-Segmented Polydiacetylenes

Keda Hu,¹ Elena Pandres,² Yang Qin¹

¹Department of Chemistry and Chemical Biology, University of New Mexico, MSC03 2060, 1 UNM, Albuquerque, New Mexico 87131

²Department of Chemical Engineering, University of Massachusetts, Amherst, Massachusetts 01003

Correspondence to: Y. Qin (E-mail: yangqin@unm.edu)

Received 25 March 2014; accepted 10 June 2014; published online 20 June 2014

DOI: 10.1002/pola.27286

ABSTRACT: We report the synthesis and characterization of a novel series of platinum-segmented polydiacetylenes (Pt-PDAs). These polymers can be considered PDAs having every other double bond replaced with a Pt center and fully conjugated side groups attached to the remaining double bonds. Physical, optical and electronic properties of these polymers can be systematically tuned by changing the side groups from

alkyl to phenyl and to thienyl moieties. Application of these polymers in solution-processed organic photovoltaic devices is attempted and evaluated. © 2014 Wiley Periodicals, Inc. *J. Polym. Sci., Part A: Polym. Chem.* **2014**, 52, 2662–2668

KEYWORDS: conjugated polymers; metal-polymer complexes; organic photovoltaics; side chain conjugation; synthesis

INTRODUCTION Conjugated polymers (CPs) have attracted tremendous research interests and found widespread applications in modern electronic devices.¹ Among an overwhelmingly large amount of examples, polydiacetylenes [PDAs, Scheme 1(A)] represent one of the prototypical and unique classes of CPs since the initial discovery in 1969.² PDAs are considered quasi one-dimensional semiconductors having macroscopic long-range coherence and anisotropy, which undergo intriguing optical changes among blue, red and yellow phases upon exposure to external stimuli.³ PDAs have found applications in nonlinear optics,⁴ organic conductors,⁵ and most widely, as sensory materials.⁶ However, PDAs have rarely been applied in solution processed organic electronic devices. Stringent geometrical requirements during the commonly applied topochemical solid-state synthesis severely limit structural variations of substituents directly attached to the polymer backbone.^{3(a),7} Electronic properties of resulting PDAs are thus difficult to modify through substituent variation and the polymers usually have limited solubility, making integration of these materials into solution-fabricated electronic devices challenging. We have recently developed a facile synthetic methodology toward functionalized enediyne [EDY, Scheme 1(B)] molecules.⁸ Following methylation of these terminal alkynes, PDAs having directly attached aromatic groups as well as tunable electronic properties were obtained via a novel acyclic enediyne metathesis polymerization technique.

Incorporation of transition metals into CP frameworks is another intriguing strategy to adjust polymer electronic fea-

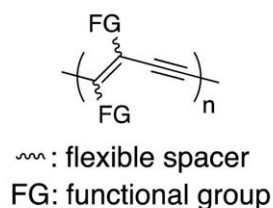
tures and result in properties characteristic to metals.⁹ Platinum-containing CPs are a commonly encountered class of such metal incorporated polymers, which have been applied frequently in organic photovoltaics (OPVs).¹⁰ Typical Pt-containing polymers have the Type I structures shown in Scheme 1(C), in which the organic chromophores feature several electron-rich and -poor aromatic moieties connected in series along the main chain direction.¹¹ In such donor-acceptor design, chromophores typically contain several aromatic rings side-by-side and are relatively long. The increased chromophore length can potentially dilute Pt-induced spin-orbit coupling effects and lower triplet generation yields that have been considered beneficial for OPV operations.¹² For this regard, the Type II structure shown in Scheme 1(C) can be especially interesting, in which chromophores are connected through the short axis and the distance between chromophore and Pt centers is greatly reduced. Such structural motif has yet to be studied in detail for Pt-containing CPs.

We report herein the synthesis and characterization of a series of Pt-segmented PDAs (Pt-PDAs) as shown in Scheme 1(D). These structures can be considered as PDAs having every other double bond replaced by a Pt center. The remaining double bonds bear two functional groups that are fully conjugated with each other and with the main chain, leading to the Type II structure discussed above. Impacts on polymer properties and OPV device performance with such structural design, that is, Pt incorporation and chromophore

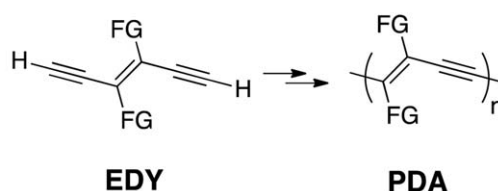
Additional Supporting Information may be found in the online version of this article.

© 2014 Wiley Periodicals, Inc.

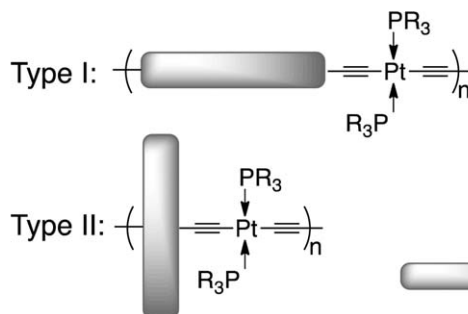
(A) Polydiacetylene (PDA)



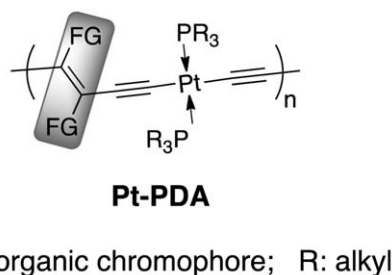
(B) Eneidyne Monomer



(C) Platinum Containing Polymer



(D) Platinum Segmented PDA



SCHEME 1 Overview.

conjugation perpendicular to polymer main chain, are carefully explored.

EXPERIMENTAL

Materials and General Methods

All reagents and solvents were used as received from Sigma-Aldrich or VWR unless otherwise noted. Phenyl-C61-butyric acid methyl ester (PCBM, >99.5%) was purchased from American Dye Source. Triisopropyl((trimethylsilyl)ethynyl)silane (**M1**) was synthesized as described previously.¹³ THF was distilled from Na/benzophenone before use. Anhydrous dichloromethane was obtained by distillation over CaH₂ and degassed through several freeze-pump-thaw cycles. The 300.13 MHz ¹H, 75.48 MHz ¹³C NMR, and 121.5 MHz ³¹P NMR spectra were recorded on a Bruker Avance III Solution 300 spectrometer. All solution ¹H and ¹³C NMR spectra were referenced internally to the tetramethylsilane peaks. Size exclusion chromatography (SEC) analyses were performed in chloroform with 0.5% (v/v) triethylamine (1 mL/min) using a Waters Breeze system equipped with a 2707 autosampler, a 1515 isocratic HPLC pump, and a 2414 refractive index detector. Two styragel columns (Polymer Laboratories; 5 μm Mix-C), which were kept in a column heater at 35 °C, were used for separation. The columns were calibrated with polystyrene standards (Varian). Ultraviolet-visible (UV-vis) absorption spectra were recorded on a Shimadzu UV-2401 PC spectrometer over a wavelength range of 250–800 nm. Fluorescence emission spectra were obtained using a Varian Cary Eclipse Fluorometer. Differential scanning calorimetry (DSC) measurements were performed on a Mettler Toledo DSC STAR[®] system with about 5–10 mg sample and at a scan

rate of 10 °C/min. The results reported are from the second heating cycle. Cyclic Voltammetry was performed at 25 °C on a CH Instrument CHI604xD electrochemical analyzer using a glassy carbon working electrode, a platinum wire counter electrode and a Ag/AgCl reference electrode calibrated using ferrocene redox couple (4.8 eV below vacuum).

Solar Cell Fabrication and Testing

ITO-coated glass substrates (China Shenzhen Southern Glass Display, 8 Ω/□) were cleaned by ultrasonication sequentially in detergent, DI water, acetone and isopropyl alcohol, each for 15 min followed by UV-ozone treatment (PSD Series, Novascan) for 45 min. MoO₃ (10 nm) was deposited inside an glovebox integrated Angstrom Engineering Åmod deposition system at a base vacuum level <7 × 10^{−8} Torr. Polymer/PCBM blend solutions were then spun-cast at predetermined speeds using a glovebox integrated spin coater (Special Coating Systems, SCS-G3). Al (100 nm) was lastly thermally evaporated through patterned shadow masks. Current-voltage (I-V) characteristics were measured by a Keithley 2400 source-measuring unit under simulated AM1.5G irradiation (100 mW cm^{−2}) generated by a Xe arc-lamp based Newport 67005 150-W solar simulator equipped with an AM1.5G filter (Newport). The light intensity was calibrated using a Newport thermopile detector (model 818P-010-12) equipped with a Newport 1916-C Optical Power Meter.

1-(Thiophen-2-yl)-3-(triisopropylsilyl)prop-2-yn-1-one (**M2**)

To a suspension of AlCl₃ (7.36 g, 55.2 mmol) in 200 mL hexanes was added triisopropyl((trimethylsilyl)ethynyl)silane

(11.72 g, 46.0 mmol) and thiophene-2-carbonyl chloride (6.95 g, 47.4 mmol) at 0 °C. After stirring for 45 min at 0 °C and 3 h at room temperature, the reaction was quenched with water and ice mixture. The reaction mixture was extracted with hexanes twice. The organic phase was combined, washed with saturated NaHCO₃ solution and saturated brine, and dried with anhydrous Na₂SO₄. After removal of solvents, the crude product was recrystallized in methanol at −20 °C to afford **M2** as a light yellow solid (12.2 g, 90.1%). ¹H NMR (300.13 MHz, CDCl₃): δ (ppm) = 1.12–1.34 (m, 21H), 7.16 (dd, 1H, $J_{\text{HH}}^3 = 4.8$ and 3.6 Hz), 7.70 (d, 1H, $J_{\text{HH}}^3 = 4.8$ Hz), 7.94 (d, 1H, $J_{\text{HH}}^3 = 3.6$ Hz). ¹³C NMR (75.48 MHz, CDCl₃): δ (ppm) = 10.1, 18.4, 96.3, 102.5, 128.3, 134.8, 135.1, 144.8, 169.0.

(E)-(3,4-Di(thiophen-2-yl)hexa-3-en-1,5-diyne-1,6-diyl)bis(triisopropylsilane) (M3)

To a suspension of zinc powder (5.10 g, 78.0 mmol) in 300-mL dry THF was added TiCl₄ (4.22 mL, 38.9 mmol) drop wise at 0 °C under nitrogen. The mixture was heated to reflux for 5 h till a dark solution was obtained, and then cooled down to 0 °C. Compound **M2** (7.50 g, 25.7 mmol) and pyridine (2.50 mL, 28.3 mmol) was added through a degassed syringe and the reaction mixture was refluxed for another 24 h. The reaction was quenched with saturated sodium bicarbonate, extracted with ethyl ether twice. The combined organic phase was washed with saturated brine and dried with anhydrous Na₂SO₄. Compound **M3** was recrystallized in hexane and ethanol at −20 °C as a light brown solid (3.50 g, 49.3%).

¹H NMR (300.13 MHz, CDCl₃): δ (ppm) = 1.11–1.23 (m, 42H), 7.00 (dd, 2H, $J_{\text{HH}}^3 = 5.1$ and 3.9 Hz), 7.31 (d, 2H, $J_{\text{HH}}^3 = 5.1$ Hz), 8.00 (d, 2H, $J_{\text{HH}}^3 = 3.9$ Hz). ¹³C NMR (75.48 MHz, CDCl₃): δ (ppm) = 11.4, 18.7, 106.2, 106.4, 118.8, 126.5, 126.8, 129.3, 142.2.

(E)-1,1'-(5,5'-(1,6-Bis(triisopropylsilyl)hexa-3-en-1,5-diyne-3,4-diyl)bis(thiophene-5,2-diyl))bis(dodecan-1-one) (M4)

To a suspension of AlCl₃ (0.600 g, 4.50 mmol) in 20-mL dry dichloromethane was added dodecanoyl chloride (1.29 mL, 5.40 mmol) and compound **M3** (1.01 g, 1.81 mmol) at 0 °C. After stirring for 45 min at 0 °C and 12 h at room temperature, the reaction was quenched with water and ice mixture, extracted with hexanes twice. The organic layer was combined, washed with saturated NaHCO₃ solution, saturated brine and dried with anhydrous Na₂SO₄. Compound **M4** was passed through a silica gel column (eluent CH₂Cl₂) and then recrystallized in hexane at −20 °C as a red solid (0.83 g, 50.0%).

¹H NMR (300.13 MHz, CDCl₃): δ (ppm) = 0.88 (t, 6H, $J_{\text{HH}}^3 = 6.6$ Hz), 1.11–1.24 (m, 42H), 1.26–1.33 (m, 32H), 1.72 (m, 4H), 2.86 (t, 4H, $J_{\text{HH}}^3 = 7.5$ Hz), 7.62 (d, 2H, $J_{\text{HH}}^3 = 3.9$ Hz), 7.96 (d, 2H, $J_{\text{HH}}^3 = 3.9$ Hz). ¹³C NMR (75.48 MHz, CDCl₃): δ (ppm) = 11.3, 14.1, 18.7, 22.7, 24.8, 29.3, 29.4, 29.5, 29.6, 31.9, 39.6, 104.7, 110.5, 120.4, 130.6, 130.9, 144.0, 148.6, 193.5.

(E)-1,1'-(5,5'-(Hexa-3-en-1,5-diyne-3,4-diyl)bis(thiophene-5,2-diyl))bis(dodecan-1-one) (EDY-Th)

To a solution of **M4** (2.00 g, 2.20 mmol) in 40 mL THF was added tetrabutylammonium fluoride (1 M in THF, 8.80 mL, 8.80 mmol) and 1 mL water. The mixture was stirred overnight at room temperature. The reaction mixture was then extracted with ethyl ether twice, washed with saturated brine and dried over anhydrous Na₂SO₄. After removal of solvent, the crude product was passed through a silica gel column (eluent CH₂Cl₂) and then recrystallized in hexane and chloroform at −20 °C to afford **EDY-Th** as a yellow powder (1.10 g, 83.3%).

¹H NMR (300.13 MHz, CDCl₃): δ (ppm) = 0.88 (t, 6H, $J_{\text{HH}}^3 = 6.6$ Hz), 1.26–1.33 (m, 32H), 1.72 (m, 4H), 2.89 (t, 4H, $J_{\text{HH}}^3 = 7.5$ Hz), 4.07 (s, 2H), 7.62 (d, 2H, $J_{\text{HH}}^3 = 4.2$ Hz), 7.88 (d, 2H, $J_{\text{HH}}^3 = 4.2$ Hz). ¹³C NMR (75.48 MHz, CDCl₃): δ (ppm) = 14.1, 22.7, 24.8, 29.3, 29.4, 29.5, 29.6, 31.9, 39.4, 81.8, 93.7, 120.5, 130.7, 131.6, 144.7, 147.4, 193.9.

General Procedure for the Synthesis of Pt-PDAs Using Pt-PDA-CH as a Representative

The reaction was set up in a glovebox under Argon. To a solution of 0.20 mmol **EDY-CH** monomer and 0.20 mmol *trans*-Pt(PET₃)₂Cl₂ was added 19 mg CuI (0.10 mmol), 10 mL dry CH₂Cl₂, and 3 mL dry triethylamine. After stirring at room temperature for 24 h under argon, the reaction was quenched by exposing to air. The reaction mixture was concentrated to about 0.7 mL, and then added dropwise to 30 mL methanol for precipitation. The polymers were collected by filtration, washed with methanol and dried under high vacuum.

Pt-PDA-CH

Pt-PDA-CH was isolated as a yellow waxy solid (80 mg, 82.9%).

¹H NMR (300.13 MHz, CDCl₃): δ (ppm) = 0.88, 1.09–1.17, 1.25, 1.51, 2.07, 2.38. ¹³C NMR (75.48 MHz, CDCl₃): δ (ppm) = 8.26, 14.1, 15.9, 16.1, 16.3, 22.7, 29.4, 29.7, 29.8, 29.9, 30.1, 31.9, 36.7, 127.1. ³¹P NMR (121.5 MHz, CDCl₃): δ (ppm) = 12.20 ($J_{\text{P-Pt}} = 2425$ Hz). SEC (CHCl₃, 1 mL/min): $M_n = 11.9$ kDa, $M_w = 23.8$ kDa, $PDI = 2.0$.

Pt-PDA-Ph

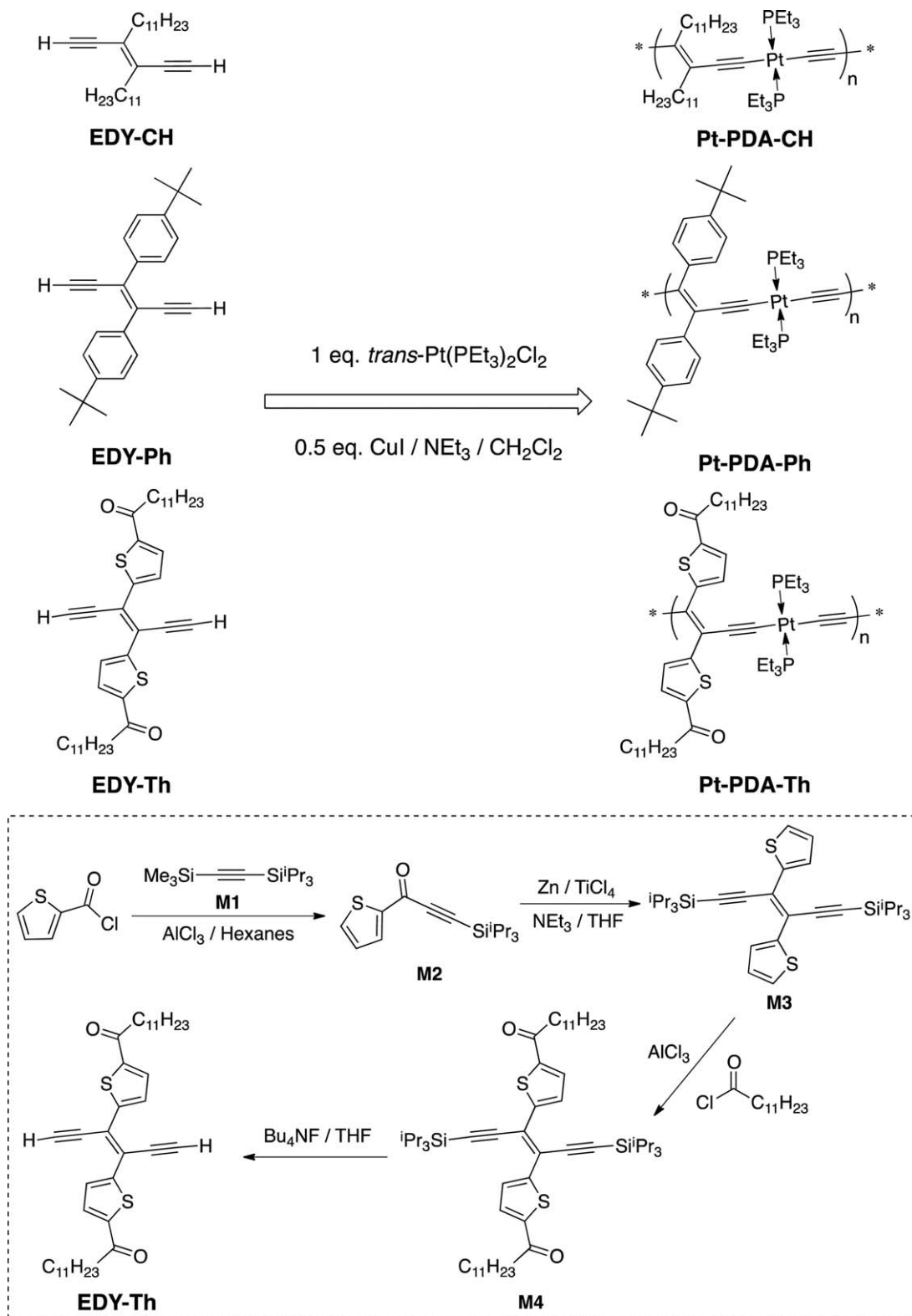
Pt-PDA-Ph was isolated as a yellow powder (20 mg, 88.5%).

¹H NMR (300.13 MHz, CDCl₃): δ (ppm) = 0.74, 0.92, 1.25, 1.44, 1.72–1.83. ¹³C NMR (75.48 MHz, CDCl₃): δ (ppm) = 8.2, 15.7, 31.4, 34.4, 123.7, 128.9. ³¹P NMR (121.5 MHz, CDCl₃): δ (ppm) = 11.96 ($J_{\text{P-Pt}} = 2349$ Hz). SEC (CHCl₃, 1 mL/min): $M_n = 12.3$ kDa, $M_w = 22.1$ kDa, $PDI = 1.8$.

Pt-PDA-Th

Pt-PDA-Th was isolated as a red powder (34 mg, 95.0%).

¹H NMR (300.13 MHz, CDCl₃): δ (ppm) = 0.87, 1.19–1.26, 1.78, 2.12, 2.91, 7.68, 8.43. ¹³C NMR (75.48 MHz, CDCl₃): δ (ppm) = 8.5, 14.1, 16.1, 16.3, 16.6, 22.7, 25.2, 29.4, 29.6,



SCHEME 2 Synthesis of monomers and polymers.

29.7, 31.9, 39.4, 131.4, 141.6, 154.7, 193.8. ³¹P NMR (121.5 MHz, CDCl₃): δ (ppm) = 12.56 (*J*_{P-Pt} = 2341 Hz). SEC (CHCl₃, 1 mL/min): *M*_n = 13.1 kDa, *M*_w = 27.6 kDa, *PDI* = 2.1.

RESULTS AND DISCUSSION

Synthesis of EDY monomers and Pt-PDA polymers are summarized in Scheme 2. Preparation of **EDY-CH** and **EDY-Ph** was described previously⁸ and **EDY-Th** was synthesized

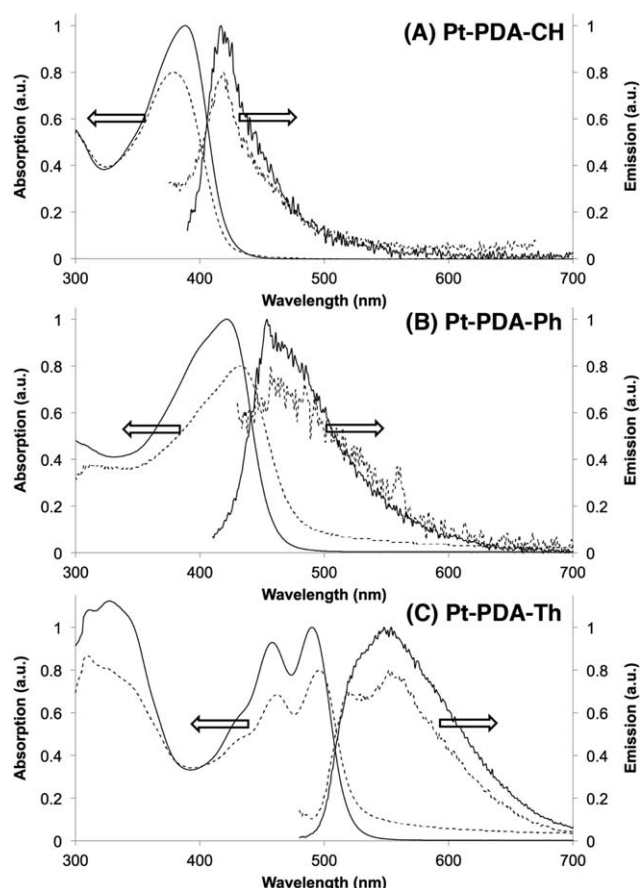


FIGURE 1 Normalized absorption and emission spectra of **Pt-PDA-CH**, **Pt-PDA-Ph**, and **Pt-PDA-Th** in CHCl_3 solutions (10^{-5} M repeating units, solid lines) and thin films spun cast from CHCl_3 solutions (ca. 1 mg/mL) onto commercial ITO/glass substrates (dashed lines).

similarly from commercially available thiophene-2-carbonyl chloride. In order to impart good solubility to resulting polymers, long alkyl side chains are the most commonly applied strategy. Attempts to install linear alkyl substituents at the 5-thienyl positions of **M3**, including lithiation followed by SN_2 reaction with alkyl halides and halogenation followed by cross-coupling with alkyl Grignard reagents, failed to generate the desired products. Instead, acylation under Friedel-Crafts conditions led smoothly to **M4** that was easily con-

verted to **EDY-Th** via desilylation. Polymerization was conducted by combining these EDY monomers with equimolar *trans*- $\text{Pt}(\text{PET}_3)_2\text{Cl}_2$, respectively, in the presence of CuI and NEt_3 in CH_2Cl_2 , which led to corresponding Pt-PDAs in high yields. The polymers were purified by precipitation into and extraction with methanol, and were extensively dried under high vacuum. New reaction intermediates and resulting polymers were fully characterized by NMR spectroscopy, which supports proposed structures and matches those of related compounds reported previously.^{8,14} Molecular weights of the Pt-PDA polymers were estimated by SEC against polystyrene standards. All three polymers showed mono-modal profiles (Supporting Information Fig. S1) and similar M_n 's of 11.9, 12.3 and 13.1 kDa were obtained for **Pt-PDA-CH**, **Pt-PDA-Ph**, and **Pt-PDA-Th**, respectively. Similar polydispersity indexes (PDIs) of about 2 were obtained for the polymers, which is typical of stepwise polymerization processes.

These Pt-PDAs are readily soluble in various organic solvents including CHCl_3 , toluene, chlorobenzene and THF, and so forth. **Pt-PDA-CH** appears as a yellow wax and is even soluble in hexanes, likely due to the long undecyl side chains and the absence of any rigid aromatic groups. Both **Pt-PDA-Ph** and **Pt-PDA-Th** exist as solids, the former being yellow while the later being red. Such apparently different solid-state properties were probed in more detail by DSC measurements (Supporting Information Fig. S2). A melting transition ranging from 20 to 40 °C was observed for **Pt-PDA-CH**, which is likely due to side chain melting when considering the melting point of docosane ($n\text{-C}_{22}\text{H}_{46}$) at about 40 °C. No endotherms could be observed for **Pt-PDA-Ph** from −30 to 250 °C and large, irreversible exothermic transitions appeared above about 170 °C, possibly due to polymer decomposition. Significant steric hindrance originated from bulky *tert*-butylphenyl and triethylphosphine substituents likely explains the amorphous nature and poor stability of the polymer. On the other hand, **Pt-PDA-Th**, bearing smaller and more planar acyl thienyl side groups, has a melting transition at 154–169 °C, indicating enhanced crystallinity.

Optical properties of the Pt-PDAs are evaluated by absorption and emission spectroscopy in both dilute CHCl_3 solutions and as thin films. The results are summarized in Figure 1 and Table 1, and absorption and emission spectra of corresponding EDY monomers are shown in Supporting

TABLE 1 Electronic Properties and OPV Device Parameters of Pt-PDAs

	λ_{max} (nm) ^a	λ_{em} (nm) ^b	Bandgap ^c (eV)	HOMO ^d (eV)	LUMO ^e (eV)	V_{OC} (V) ^f	J_{SC} (mA/cm ^{−2}) ^f	FF ^f	PCE (%) ^f
Pt-PDA-CH	388 (380)	417 (419)	2.9 (2.9)	−4.8	−1.9	— ^g	— ^g	— ^g	— ^g
Pt-PDA-Ph	422 (433)	454 (457)	2.7 (2.5)	−4.8	−2.1	0.65	0.61	0.38	0.15
Pt-PDA-Th	490 (497)	548 (552)	2.4 (2.3)	−5.2	−2.8	0.79	0.69	0.47	0.26

^a CHCl_3 solutions (ca. 10^{-5} M), thin film data in parentheses.

^b Excited at λ_{max} , CHCl_3 solutions (ca. 10^{-5} M), thin film data in parentheses.

^c Optical bandgap estimated from absorption edge, thin film data in parentheses.

^d Estimated from electrochemical oxidation onset in CH_2Cl_2 solution.

^e Obtained from the difference between HOMO and optical bandgap in solution.

^f Average of five devices.

^g Not tested, see text.

Information Figure S3. As seen in Figure 1, optical properties of Pt-PDAs are clearly tunable by variation of functional groups directly attached to the main chain double bonds. Both absorption and emission maxima red shift to longer wavelengths through replacing alkyl substituents with aromatic groups. The red-shift is more pronounced in **Pt-PDA-Th** due to the less aromatic, and thus more delocalized, thiophene moieties and electron withdrawing carbonyl groups. Such effect is further confirmed by cyclic voltammetry as shown in Supporting Information Figure S4. All three polymers showed multiple irreversible oxidation events and two common oxidation peaks having onsets at about 1.05 and 1.34 V (against Ag/AgCl reference electrode) are observed for all polymers. These are ascribed to stepwise two-electron oxidations at the platinum centers, consistent with previous literature reports.¹⁵ As expected, the first oxidation potentials are different due to the various extent of side chain conjugation in these polymers, which can be conveniently used to estimate the polymers' HOMO energy levels. While both **Pt-PDA-CH** and **Pt-PDA-Ph** have similar HOMO energy levels at about -4.8 eV, **Pt-PDA-Th** has a deeper lying HOMO level at about -5.2 eV. No reduction events could be observed for all three polymers within the experimental electrochemical window and the LUMO levels were thus estimated from the optical bandgaps (Table 1).

Pt-PDA-CH exhibits structureless absorption and emission profiles while clear vibronic structures could be observed in the case of **Pt-PDA-Th**. Only slight red-shift can be observed in both absorption and emission profiles of **Pt-PDA-Ph** and **Pt-PDA-Th** compared with corresponding solution spectra, indicating an overall amorphous nature that has been observed in most other Pt-containing polymers. Interestingly, an 8-nm blue-shift is observed in the thin film absorption of **Pt-PDA-CH**, which is possibly due to side chain entanglement leading to main chain twist and reduction in conjugation lengths. Emissions of all three polymers are likely fluorescence in nature since relatively small Stoke's shifts and no emission intensity difference could be observed both in degassed and aerated solutions. Fluorescence quantum efficiencies are estimated against anthracene standards to be about 0.02, 0.2, and 0.03% for **Pt-PDA-CH**, **Pt-PDA-Ph**, and **Pt-PDA-Th**, respectively. Similarly, no fluorescence could be observed for **EDY-CH** while both **EDY-Ph** (0.13%) and **EDY-Th** (0.15%) have very low quantum efficiencies. There is thus likely an intrinsic ultra-fast excited state deactivation pathway other than Pt-induced intersystem crossing in these EDY monomers and corresponding Pt-PDA polymers, which could be similar in nature as the dark states in blue-phase PDAs.^{3(b)}

To further explore the possibility of applying these Pt-PDAs in solution processed electronic devices, bulk heterojunction (BHJ) OPVs were fabricated using these polymers and phenyl-C61-butyric acid methyl ester (PCBM) as the electron acceptor. All devices adopt the basic structure ITO/MoO₃ (10 nm)/active layer (100 nm)/Al (100 nm) and the active layer contains Pt-PDA and PCBM in a 1/2 ratio by weight.¹⁶ Devices were tested under as-cast conditions since thermal

annealing was found to degrade performance significantly. Due to the low melting point and waxy nature of **Pt-PDA-CH**, no satisfactory blend films could be obtained and photovoltaic effects could not be observed. On the other hand, devices made from **Pt-PDA-Ph** and **Pt-PDA-Th** gave average power conversion efficiencies (PCEs) of 0.15% and 0.26% (Table 1), respectively. The latter showed a 0.14 V higher open circuit voltage (V_{OC}), which correlates well with the deeper lying HOMO level of **Pt-PDA-Th**. OPVs of both polymers suffer greatly from low short circuit currents (J_{SC}) and fill factors (FFs), which can be resulted from large bandgaps, amorphous nature and short-lived excitons. We are currently optimizing these devices and studying the charge generation mechanisms in more detail.

CONCLUSIONS

In summary, we have successfully prepared a novel series of platinum segmented polydiacetylenes that bear conjugated side groups directly attached to the polymer main chains. Physical and electronic properties of resulting polymers can be systematically tuned through variation of the side groups and substituents. With proper selection of conjugated side chains, such Pt-PDA structural design can lead to polymers having interesting optical and electronic properties, and potentially finding applications in organic electronic devices including OPVs.

ACKNOWLEDGMENTS

The authors acknowledge University of New Mexico for financial support for this research. National Science Foundation (NSF) is acknowledged for supporting the NMR facility at UNM through grants CHE-0840523 and 0946690. Y. Qin acknowledges NSF Grant No. IIA-1301346 for financial support. E. Pandres thank the University of New Mexico's Nanoscience and Microsystems REU program for the research opportunity.

REFERENCES AND NOTES

- 1 Handbook of Conducting Polymers, 3rd ed.; T. A. Skotheim, J. R. Reynolds, Eds.; CRC Press: Boca Raton, **2007**.
- 2 G. Wegner, *Z. Naturforsch.* **1969**, B24, 824–832.
- 3 (a) H. Zuilhof, H. M. Barentsen, M. van Dijk, E. J. R. Sudhölter, J. O. M. Hoofman, L. D. A. Siebbeles, M. P. de Haas, J. M. Warman, In *Supramolecular Photosensitive and Electroactive Materials*; H. S. Nalwa, Ed.; Academic Press: San Diego, **2001**; (b) M. Schott, In *Photophysics of Molecular Materials*; G. Lanzani, Ed.; Wiley-VCH: Weinheim, **2006**, Chapter 3, pp 49–150; (c) R. R. Chance, R. H. Baughman, H. Müller, C. J. Eckhardt, *J. Chem. Phys.* **1977**, 67, 3616–3618; (d) S. Dei, A. Matsumoto, A. Matsumoto, *Macromolecules* **2008**, 41, 2467–2473; (e) C. Tanioku, K. Matsukawa, A. Matsumoto, *ACS Appl. Mater. Interfaces* **2013**, 5, 940–948; (f) H. Müller, C. J. Eckhardt, *Mol. Cryst. Liq. Cryst.* **1978**, 45, 313–318; (g) R. W. Carpick, D. Y. Sasaki, A. R. Burns, *Langmuir* **2000**, 16, 1270–1278; (h) B. Tieke, G. Lieser, G. Wegner, *J. Polym. Sci. Polym. Chem. Ed.* **1979**, 17, 1631–1644; (i) D. H. Charych, J. O. Nagy, W. Spevak, M. D. Bednarski, *Science* **1993**, 261, 585–588; (j) A. Reichert, J.

- O. Nagy, W. Spevak, D. H. Charych, *J. Am. Chem. Soc.* **1995**, *117*, 829–830.
- 4** (a) T. Kanetake, K. Ishikawa, T. Hasegawa, T. Koda, K. Takeda, M. Hasegawa, K. Kubodera, H. Kobayashi, *Appl. Phys. Lett.* **1989**, *54*, 2287–2289; (b) A. Sarkar, S. Okada, H. Matsuzawa, H. Matsuda, H. Nakanishi, *J. Mater. Chem.* **2000**, *10*, 819–828; (c) G.-J. Zhou, W.-Y. Wong, *Chem. Soc. Rev.* **2011**, *40*, 2541–2566; (d) G.-J. Zhou, W.-Y. Wong, Z. Lin, C. Ye, *Angew. Chem. Int. Ed.* **2006**, *45*, 6189–6193; (e) G.-J. Zhou, W.-Y. Wong, C. Ye, Z. Lin, *Adv. Funct. Mater.* **2007**, *17*, 963–975.
- 5** (a) H. Nakanishi, H. Matsuda, M. Kato, *Mol. Cryst. Liq. Cryst.* **1984**, *105*, 77–88; (b) K. Se, H. Ohnuma, T. Kotaka, *Macromolecules* **1984**, *17*, 2126–2131.
- 6** (a) H. Peng, Y. Lu, *Langmuir* **2006**, *22*, 5525–5527; (b) H. Peng, *J. Phys. Chem. B* **2007**, *111*, 8885–8890; (c) X. Sun, T. Chen, S. Huang, L. Li, H. Peng, *Chem. Soc. Rev.* **2010**, *39*, 4244–4257.
- 7** (a) T. Kim, Q. Ye, L. Sun, K. C. Chan, R. M. Crooks, *Langmuir* **1996**, *12*, 6065–6073; (b) H. M. Barentsen, M. van Dijk, P. Kimkes, H. Zuilhof, E. J. R. Sudhölter, *Macromolecules* **1999**, *32*, 1753–1762.
- 8** K. Hu, H. Yang, W. Zhang, Y. Qin, *Chem. Sci.* **2013**, *4*, 3649–3635.
- 9** (a) I. Manners, *Science* **2001**, *294*, 1664–1666; (b) R. P. Kingsborough, T. M. Swager, In *Progress in Inorganic Chemistry*; K. D. Karlin, Ed.; Wiley: Hoboken, NJ, **1999**; Vol. 48; (c) T. Hirao, *Coord. Chem. Rev.* **2002**, *226*, 81–91; (d) Y. Liu, Y. Li, K. S. Schanze, *J. Photochem. Photobiol. C Photochem. Rev.* **2002**, *3*, 1–23; (e) C. Moorlag, B. C. Sih, T. L. Stott, M. O. Wolf, *J. Mater. Chem.* **2005**, *15*, 2433–2436; (f) M. O. Wolf, *J. Inorg. Organomet. Polym. Mater.* **2006**, *16*, 189–199; (g) W.-Y. Wong, C.-L. Ho, *Coord. Chem. Rev.* **2006**, *250*, 2627–2690; (h) C.-L. Ho, W.-Y. Wong, *Coord. Chem. Rev.* **2011**, *255*, 2649–2502.
- 10** (a) W.-Y. Wong, S.-M. Chan, K.-H. Choi, K.-W. Cheah, W.-K. Chan, *Macromol. Rapid Commun.* **2000**, *21*, 453–457; (b) F. Guo, Y.-G. Kim, J. R. Reynolds, K. S. Schanze, *Chem. Commun.* **2006**, 1887–1889; (c) W.-Y. Wong, X.-Z. Wang, Z. He, K.-K. Chan, A. B. Djuricic, K.-Y. Cheung, C.-T. Yip, A. M.-C. Ng, Y. Y. Xi, C. S. K. Mak, W.-K. Chan, *J. Am. Chem. Soc.* **2007**, *129*, 14372–14380; (d) W.-Y. Wong, X. Wang, H.-L. Zhang, K.-Y. Cheung, M.-K. Fung, A. B. Djurišić, W.-K. Chan, *J. Organomet. Chem.* **2008**, *693*, 3603–3612; (e) J. Mei, K. Ogawa, Y.-G. Kim, N. C. Heston, D. J. Arenas, Z. Nasrollahi, T. D. McCarley, D. B. Tanner, J. R. Reynolds, K. S. Schanze, *ACS Appl. Mater. Interfaces* **2009**, *1*, 150–161; (f) P.-T. Wu, T. Bull, F. S. Kim, C. K. Luscombe, S. A. Jenekhe, *Macromolecules* **2009**, *42*, 671–681; (g) H. Zhan, S. Lamare, A. Ng, T. Kenny, H. Guernon, W.-K. Chan, A. B. Djurišić, P. D. Harvey, W.-Y. Wong, *Macromolecules* **2011**, *44*, 5155–5167; (h) W.-Y. Wong, *Macromol. Chem. Phys.* **2008**, *209*, 14–24; (i) W.-Y. Wong, C.-L. Ho, *Acc. Chem. Res.* **2010**, *43*, 1246–1256; (j) W.-Y. Wong, P. D. Harvey, *Macromol. Rapid Commun.* **2010**, *31*, 671–713; (k) C.-L. Ho, W.-Y. Wong, *Coord. Chem. Rev.* **2013**, *257*, 1614–1649; (l) W.-Y. Wong, *Dalton Trans.* **2007**, 4495–4510; (m) W.-Y. Wong, *J. Inorg. Organomet. Polym. Mater.* **2005**, *15*, 197–219; (n) L. Liu, C.-L. Ho, W.-Y. Wong, K.-Y. Cheung, M.-K. Fung, W.-T. Lam, A. B. Djuricic, W.-K. Chan, *Adv. Funct. Mater.* **2008**, *18*, 2824–2833.
- 11** (a) W.-Y. Wong, X.-Z. Wang, Z. He, A. B. Djuricic, C.-T. Yip, K.-Y. Cheung, H. Wang, C. S. K. Mak, W.-K. Chan, *Nat. Mater.* **2007**, *6*, 521–527; (b) N. S. Baek, S. K. Hau, H.-L. Yip, O. Acton, K.-S. Chen, A. K.-Y. Jen, *Chem. Mater.* **2008**, *20*, 5734–5736; (c) X.-Z. Wang, W.-Y. Wong, K.-Y. Cheung, M.-K. Fung, A. B. Djuricic, W.-K. Chan, *Dalton Trans.* **2008**, 5484–5494; (d) X.-Z. Wang, Q. Wang, L. Yan, W.-Y. Wong, K.-Y. Cheung, A. Ng, A. B. Djuricic, W.-K. Chan, *Macromol. Rapid Commun.* **2010**, *31*, 861–867; (e) Q. Wang, W.-Y. Wong, *Polym. Chem.* **2011**, *2*, 432–440; (f) C. Qin, Y. Fu, C.-H. Chui, C.-W. Kan, Z. Xie, L. Wang, W.-Y. Wong, *Macromol. Rapid Commun.* **2011**, *32*, 1472–1477; (g) L. Y. Yan, Y. Zhao, X. Wang, X.-Z. Wang, W.-Y. Wong, Y. Liu, W. Wu, Q. Xiao, G. Wang, X. Zhou, W. Zeng, C. Li, X. Wang, H. Wu, *Macromol. Rapid Commun.* **2012**, *33*, 603–609.
- 12** (a) A. Köhler, H. F. Wittmann, R. H. Friend, M. S. Khan, J. Lewis, *Synt. Met.* **1996**, *77*, 147–150; (b) D. Beljonne, H. F. Wittmann, A. Köhler, S. Graham, M. Younus, J. Lewis, P. R. Raithby, M. S. Khan, R. H. Friend, J. L. Brédas, *J. Chem. Phys.* **1996**, *105*, 3868–3877; (c) N. Chawdhury, A. Köhler, R. H. Friend, W.-Y. Wong, J. Lewis, M. Younus, P. R. Raithby, T. C. Corcoran, M. R. A. Al-Mandhary, M. S. Khan, *J. Chem. Phys.* **1999**, *110*, 4963–4970; (d) J. S. Wilson, A. Köhler, R. H. Friend, M. K. Al-Suti, M. R. A. Al-Mandhary, M. S. Khan, P. R. Raithby, *J. Chem. Phys.* **2000**, *113*, 7627–7634; (e) Y. Liu, S. Jiang, K. Glusac, D. H. Powell, D. F. Anderson, K. S. Schanze, *J. Am. Chem. Soc.* **2002**, *124*, 12412–12413; (f) G. Ramakrishna, T. Goodson, III; J. E. Rogers-Haley, T. M. Cooper, D. G. McLean, A. Urbas, *J. Phys. Chem. C* **2009**, *113*, 1060–1066.
- 13** C. J. Helal, P. A. Magriotis, E. J. Corey, *J. Am. Chem. Soc.* **1996**, *118*, 10938–10939.
- 14** W. He, Y. Jiang, Y. Qin, *Polym. Chem.* **2014**, *5*, 1298–1304.
- 15** M. Younus, A. Köhler, S. Cron, N. Chawdhury, M. R. A. Al-Mandhary, M. S. Khan, J. Lewis, N. J. Long, R. H. Friend, P. R. Raithby, *Angew. Chem. Int. Ed.* **1998**, *37*, 3036–3039.
- 16** We have also experimented using the commonly applied PEDOT:PSS as the anode interfacial layer while keeping other fabrication parameters constant. All devices under test showed very low efficiencies that are strongly limited by reduced open circuit voltage (Voc) values at 0.4 V for **Pt-PDA-Ph** and 0.14 V for **Pt-PDA-Th**, respectively. Such low Voc values indicate non-Ohmic contacts between the anode and the active layer, as well as possible current leakage by using PEDOT:PSS, which is consistent with our previous observations in OPVs employing similar Pt-containing polymers.¹⁴